

Proposal:	4-01-1253	Council:	10/2012	
Title:	Anomalous spin response in noncentrosymmetric systems			
This proposal is a new proposal				
Research Area:	Physics			
Main proposer:	FAK Bjorn			
Experimental Team:	FAK Bjorn ADROJA Devashibhai T.			
Local Contact:	BOEHM Martin			
Samples:	CePt3Si			
Instrument	Req. Days	All. Days	From	To
IN14	7	5	24/05/2013	29/05/2013
Abstract: We propose to measure the momentum dependence of the anomalous spin susceptibility in the noncentrosymmetric heavy-fermion CePt3Si. Due to the antisymmetric Rashba-type spin-orbit coupling, the xx and yy components of the anomalous spin susceptibility are expected to have different wave vector dependencies, and this can be probed using polarized neutron scattering on a triple-axis spectrometer. We believe the proposed experiment represents one of the first studies of the anomalous spin susceptibility in a noncentrosymmetric system. Additionally, the experiment may give an estimate of the strength of the Rashba coupling, from which the splitting of the Fermi surfaces could be determined, and hence give further insight in the unconventional superconductivity of CePt3Si.				

Anomalous Spin Response in the Non-Centrosymmetric Metal CePt₃Si

Björn Fåk¹, Devashibhai T. Adroja², Mechthild Enderle³, Martin Böhm³,
 Gerard Lapertot¹, and Vladimir P. Mineev¹

¹SPSMS, UMR-E CEA/UJF-Grenoble 1, INAC, F-38054 Grenoble, France

²ISIS Facility, STFC Rutherford Appleton Laboratory, Chilton, Didcot, Oxon OX11 0QX, U.K.

³Institut Laue-Langevin, BP 156, F-38042 Grenoble Cedex 9, France

(Received January 17, 2014; accepted April 14, 2014; published online May 20, 2014)

Non-centrosymmetric metals with tetragonal structure are characterized by an antisymmetric Rashba-type spin-orbit interaction, which has been predicted to give rise to anomalous spin susceptibility. Our polarized inelastic neutron scattering measurements in the normal phase of the heavy-fermion superconductor CePt₃Si confirm this prediction. We find that for a finite wave vector along the crystallographic *a*-direction the spin susceptibility χ_{aa} is different from χ_{bb} by a factor of two. The effect is even larger than in theoretical calculations based on the Hubbard model, and we speculate that this is due to the strong spin-orbit coupling of rare-earth heavy fermions.

The lack of inversion symmetry in a crystallographic structure may lead to surprising and non-trivial effects.^{1–3} In metallic systems, the absence of inversion center leads to an antisymmetric spin-orbit coupling that splits the Fermi surface and removes the spin degeneracy of the electronic states. Such systems may develop unconventional superconductivity at low temperatures with mixed spin-singlet and spin-triplet Cooper pairing channels.^{4,5} Unusual effects are also expected in the *normal state*, where in particular the static spin susceptibilities are predicted to be anomalous.⁶ In a non-centrosymmetric tetragonal system, it has been predicted that the static spin susceptibilities $\chi_{aa}(\mathbf{q})$ and $\chi_{bb}(\mathbf{q})$ would have different momentum \mathbf{q} dependencies while off-diagonal spin susceptibilities like $\chi_{ac}(\mathbf{q})$ would not vanish.⁶ This at first surprising theoretical prediction spurred us to investigate the normal phase of the archetype non-centrosymmetric tetragonal superconductor CePt₃Si using inelastic neutron scattering of polarized neutrons. In this letter, we show experimentally that the dynamic magnetic susceptibility χ_{aa} is indeed different from χ_{bb} for finite \mathbf{q} values in CePt₃Si.

CePt₃Si crystallizes in the non-centrosymmetric *P4mm* (No. 99) tetragonal space group with lattice parameters $a = 4.072$ and $c = 5.442$ Å.⁷ Inversion symmetry is broken by the absence of a mirror plane perpendicular to the *c*-axis. This causes an asymmetry in the crystal electric field potential perpendicular to the tetragonal *a*–*b* plane, which in turn leads to an antisymmetric spin-orbit coupling of Rashba type.⁸ This asymmetry does not affect the crystal field levels, and the Hund's rule $J = 5/2$ ground state of the Ce³⁺ ion is hence split by the tetragonal crystal field into three Kramers doublets in the usual way. The ground-state doublet is $0.46|\pm 5/2\rangle + 0.89|\mp 3/2\rangle$.⁹ Antiferromagnetic (AFM) collinear order sets in at $T_N = 2.2$ K with a propagation vector of $\mathbf{k} = (0, 0, 1/2)$ and a reduced moment of $0.16 \mu_B$, while unconventional superconductivity coexists with AFM order below $T_c = 0.75$ K.^{10,11} In the paramagnetic state, the energy of the spin fluctuations observed by inelastic neutron scattering are of the order of the Kondo temperature, $T_K \sim 10$ K.¹² Below T_N , the intensity of these spin fluctuations is enhanced near the antiferromagnetic propagation vector and they become dispersive across the Brillouin zone, but remain considerably broader in energy than expected for normal spin waves.¹²

Inelastic neutron scattering measurements using polarized neutrons were performed on the triple-axis spectrometer IN14 at the Institut Laue-Langevin. Monochromatic neutrons from a PG(002) crystal were polarized by a supermirror bender and focused vertically on the sample. A horizontally focusing Heusler alloy crystal was used to analyze the polarization of the scattered neutrons with a final energy of 4.36 meV and an energy resolution of 0.14 meV (full width at half maximum). The polarization \mathbf{P} of the neutron beam, determined to be $|\mathbf{P}| = 96.5\%$ from the measured flipping ratio of nuclear Bragg peaks from the sample, was manipulated by a set of four coils mounted in a “Helmholtz” geometry around the sample so that \mathbf{P} was either (i) parallel to the wave vector transfer \mathbf{Q} , (ii) perpendicular to \mathbf{Q} in the horizontal scattering plane, or (iii) perpendicular to \mathbf{Q} and to the scattering plane. The corresponding directions are referred to as *x*, *y*, and *z* in a right-handed cartesian coordinate system (see Fig. 1). Spin flippers mounted before and after the sample were used to reverse the neutron spin direction. Second-order neutrons, which are unpolarized, were removed by a liquid-nitrogen cooled Be filter mounted between the sample and the analyzer. A cylindrical single crystal of CePt₃Si, the same as used in Refs. 9 and 12, was mounted in an orange cryostat with the *b*-axis vertical, which gives access to wave vectors $\mathbf{Q} = (h, 0, l)$. Since the cylinder axis coincides with the vertical *b*-axis, absorption corrections are negligible.

In the chosen set-up, shown in Fig. 1, the intensities of the magnetic scattering polarized along the *y*- and *z*-directions, I_y and I_z , are extracted from the differences between the scattering cross-sections with neutron polarization along *x* and *y* and along *x* and *z*, respectively. Most measurements were performed using the spin-flip cross-sections along *x*, *y*, and *z*; a few measurements using the non spin-flip cross-sections were used to verify the results. It is straightforward to show that

$$I_z(h, 0, l) = S_{bb}(h, 0, l) \quad (1)$$

and

$$I_y(\pm h, 0, l) = \cos^2 \theta S_{aa}(h, 0, l) + \sin^2 \theta S_{cc}(h, 0, l) \mp 2 \cos \theta \sin \theta S_{ac}(h, 0, l), \quad (2)$$

where θ is the angle between the wave-vector transfer $\mathbf{Q} = (h, 0, l)$ and the tetragonal *c*-axis and $S_{\alpha\beta}$ is the dynamic structure factor (or scattering function) for the α, β spin components along the crystallographic axes *a*, *b*, and *c*. The

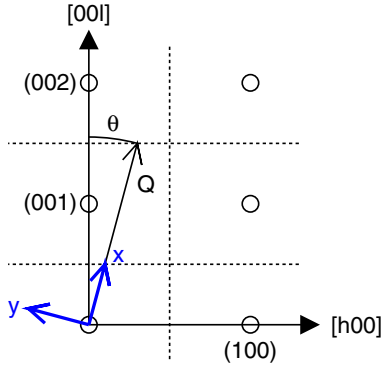


Fig. 1. (Color online) Definition of the angle θ and the (xyz) coordinate system (with z being vertical out of the plane) in the $(h0l)$ reciprocal lattice plane of CePt_3Si .

scattering function is related to the dynamic spin susceptibility via

$$S_{\alpha\alpha}(\mathbf{Q}, \omega) \propto \chi''_{\alpha\alpha}(\mathbf{Q}, \omega) F^2(\mathbf{Q}) (n_\omega + 1) \quad (3)$$

and

$$S_{\alpha\beta}(\mathbf{Q}, \omega) \propto i[\chi_{\alpha\beta}(\mathbf{Q}, \omega) - \chi_{\beta\alpha}^*(\mathbf{Q}, \omega)] F^2(\mathbf{Q}) (n_\omega + 1), \quad (4)$$

where $F(\mathbf{Q})$ is the magnetic form factor, $n_\omega = [\exp(\hbar\omega/k_B T) - 1]^{-1}$ the Bose factor, and $''$ denotes the imaginary part. The real part of the static spin susceptibility, $\chi'(\mathbf{Q})$, can in principle be obtained from the imaginary part, $\chi''(\mathbf{Q}, \omega)$, via the Kramers–Kronig relation. In practice, such an approach is too time consuming, since the intensity of the spin fluctuations in CePt_3Si is very weak. However, the spin fluctuations in CePt_3Si are well described by a Lorentzian line shape, for which the relation between $\chi'(\mathbf{Q})$ and the peak height of $\chi''(\mathbf{Q}, \omega)$ or $S(\mathbf{Q}, \omega)$ is known. A good experimental determination of $\chi'(\mathbf{Q})$ is therefore obtained within a scale factor by measuring the intensity of $\chi''(\mathbf{Q}, \omega)$ at the peak position, known from previous measurements.¹²⁾ This scale factor drops out when determining the anisotropy, since the latter is a relative quantity in the intensities. For intensity reasons, most of the measurements were performed in the ordered state, where the spin-fluctuation scattering is enhanced due to the magnetic exchange interactions but the width of the response remains similar to the paramagnetic state (see Fig. 2). This point will be discussed further below. Measurements were performed for different values of the h component of the wave vector $\mathbf{Q} = (h, 0, l)$ [in reciprocal lattice units], covering the whole Brillouin zone in this direction. Half-integer values of l , $l = 1/2$ and $3/2$, were chosen to maximize the scattering intensity due to the antiferromagnetic exchange interactions. At each h value, the energy transfer $\hbar\omega$ was adjusted within the range $0.4 \leq \hbar\omega \leq 0.7$ meV to give the maximum intensity of the inelastic scattering, known from previous measurements.¹²⁾

Inspection of Eq. (2) shows that the off-diagonal scattering, $S_{ac}(h, 0, l)$, can be eliminated by taking the average of measurements made at $+h$ and $-h$. Both χ_{aa} and χ_{cc} can be extracted from Eq. (2) by measuring at two different values of l (and hence two different values of θ) for which the spin susceptibilities are identical (such as $l = 1/2$ and $3/2$), after correction for the $|\mathbf{Q}|$ -dependent magnetic form factor $F(\mathbf{Q})$ of the Ce^{3+} ion.¹³⁾

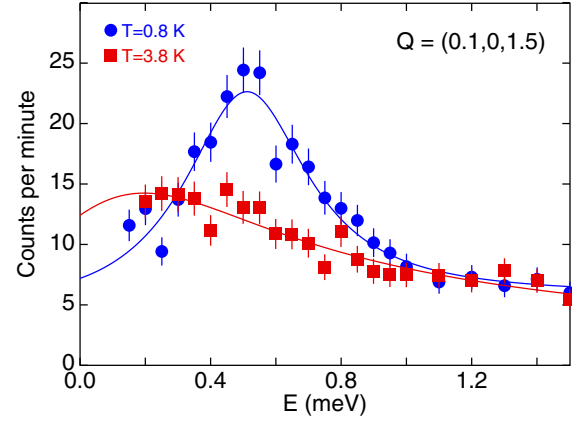


Fig. 2. (Color online) Energy scan of the scattering of unpolarized neutrons in the ordered state at $T = 0.8$ K (blue circles) and in the paramagnetic state at $T = 3.8$ K (red squares) near the antiferromagnetic zone center of CePt_3Si (from Ref. 12).

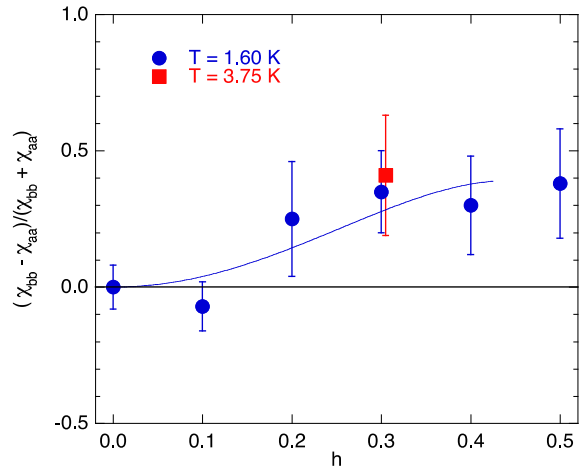


Fig. 3. (Color online) Wave vector dependence along h at $\mathbf{Q} = (h, 0, l/2)$ of the anisotropy of the magnetic susceptibilities at $T = 1.6$ K (blue circles) and $T = 3.75$ K (red square). The line is a guide to the eye based on the theoretical leading $Aq^2 + Bq^4$ dependence of the anisotropy.

The main results for the measured anisotropy of the magnetic susceptibilities are shown in Fig. 3. The figure shows the difference between χ_{bb} and χ_{aa} , normalized to their sum. The anisotropy between χ_{aa} and χ_{bb} vanishes at $h = 0$, as required by symmetry. In fact, it is the non-zero value of \mathbf{Q} along h that “breaks” the symmetry between the χ_{aa} and χ_{bb} components. For values of h larger than 0.2, the observed χ_{bb} is larger than χ_{aa} , in qualitative agreement with the calculations by Takimoto,⁶⁾ but the effect is more pronounced in the measurements. The statistical quality of the data does not allow to infer whether the anisotropy changes sign at intermediate values of h . The wave-vector dependence of the anisotropy in the spin susceptibility will be discussed in the theory part further below.

The χ_{cc} spin susceptibility evaluated from Eq. (2) has limited precision because \mathbf{Q} is close to the c -axis in our measurements and neutrons do not observe magnetic fluctuations parallel to \mathbf{Q} . The off-diagonal scattering, $S_{ac}(h, 0, l)$, obtained from Eq. (2) by taking the difference between $I_y(-h, 0, l)$ and $I_y(+h, 0, l)$, is zero within the